A Numerical Study of the Downstream Development of a Baroclinic Instability

Daniel Mukiibi

August 16, 2015

Abstract

The downstream development of baroclinic instability is studied in a 2-layer non-linear Quasi-Geostrophic (QG) model with a semi-infinite downstream extense and rigid meridional walls. Starting with a baroclinic current in a channel, a perturbation is invoked at the entrance of the channel upstream and its spatial and temporal downstream development is studied. For matters of simplicity, the study considers 2 y-modes which offers two advantages: it's simple enough to follow the 2 modes easily, and it also gives insight into the more complicated scenario of having more than a mode leading to interaction of the different modes and hence modifying the dynamics of the flow. The boundary condition at the channel entrance upstream is a temporally oscillating perturbation at $x = 0$; downstream, the potential vorticity is zero at $x = \infty$. In the $y-$direction, the derivatives of the stream function (i.e velocity) at the meridional walls are zero.

It has been found by Pedlosky (2011) that in a simple finite amplitude model of a spatially developing baroclinic instability, there's a regime during which the spatial and temporal evolution of the instability amplitude along x, t characteristics exhibits chaotic behaviour. This chaotic behaviour resulting from periodic initial conditions at the channel entrance leads to sharp and abrupt spatial variations downstream. In the current study, the non-linear development of a baroclinic instability is studied numerically in a slightly more complicated but compelling manner. In the current study, persistence of these features and the circumstances over which this behaviour persists in a more realistic oceanic model forms the main motivation for the study.

The Model

Consider the Quasi-Geostrophic(QG) equations for a two-layer model similar to the one studied in (Pedlosky, 1970) and (Pedlosky, 2011). Here, the formulation will be given in terms of the potential vorticity, q. The equations of motion in the two layers are given as below:

$$\left(\frac{\partial}{\partial t}+\mathrm{U}_1\frac{\partial}{\partial x}\right)q^{(1)}+Q_{y1}\frac{\partial\psi^{(1)}}{\partial x}+\mathrm{J}(\psi^{(1)},q^{(1)})=-r\nabla^2\psi^{(1)}. \tag{1}$$

$$\left(\frac{\partial}{\partial t}+\mathrm{U}_2\frac{\partial}{\partial x}\right)q^{(2)}+Q_{y2}\frac{\partial\psi^{(2)}}{\partial x}+\mathrm{J}(\psi^{(2)},q^{(2)})=-r\nabla^2\psi^{(2)}. \tag{2}$$

Where the jacobian, J, is defined as $J(a,b)=\dfrac{\partial a}{\partial x}\dfrac{\partial b}{\partial y}-\dfrac{\partial b}{\partial x}\dfrac{\partial a}{\partial y}$ and for a channel with no topography as is the case in this study,

$$Q_1=\nabla^2\psi_1-\mathrm{F}_1(\psi_1-\psi_2)+\beta y.$$
$$Q_2=\nabla^2\psi_1+\mathrm{F}_2(\psi_1-\psi_2)+\beta y.$$

Proposing a truncated Fourier series solution to the equations (1) and (2) of the form

$$\begin{pmatrix} q^{(1)} \\ \psi^{(1)} \end{pmatrix}=\begin{pmatrix} q_1^{(1)}(x,t)\sin\pi y+q_2^{(1)}(x,t)\sin 2\pi y+\cdots \\ \psi_1^{(1)}(x,t)\sin\pi y+\psi_2^{(1)}(x,t)\sin 2\pi y+\cdots \end{pmatrix}. \tag{3}$$

$$\begin{pmatrix} q^{(2)} \\ \psi^{(2)} \end{pmatrix}=\begin{pmatrix} q_1^{(2)}(x,t)\sin\pi y+q_2^{(2)}(x,t)\sin 2\pi y+\cdots \\ \psi_1^{(2)}(x,t)\sin\pi y+\psi_2^{(2)}(x,t)\sin 2\pi y+\cdots \end{pmatrix}. \tag{4}$$

Substituting equation (3) into equation equation (1) and projecting onto $\sin\pi y$ and $\sin 2\pi y$ yields equations (5) and (6) respectively

$$\left(\frac{\partial}{\partial t}+\mathrm{U}_1\frac{\partial}{\partial x}\right)q_1^{(1)}+Q_{y1}\frac{\partial\psi_1^{(1)}}{\partial x}-\frac{\pi^2}{2}q_2^{(1)}\frac{\partial\psi_1^{(1)}}{\partial x}+\frac{\pi^2}{4}q_1^{(1)}\frac{\partial\psi_2^{(1)}}{\partial x}\quad-$$
$$\frac{\pi^2}{4}\psi_1^{(1)}\frac{\partial q_2^{(1)}}{\partial x}+\frac{\pi^2}{2}\psi_2^{(1)}\frac{\partial q_1^{(1)}}{\partial x}=-rq_1^{(1)}. \tag{5}$$

$$\left(\frac{\partial}{\partial t}+\mathrm{U}_1\frac{\partial}{\partial x}\right)q_2^{(1)}+Q_{y1}\frac{\partial\psi_2^{(1)}}{\partial x}+\frac{\pi^2}{4}q_1^{(1)}\frac{\partial\psi_1^{(1)}}{\partial x}-\frac{\pi^2}{4}\psi_1^{(1)}\frac{\partial q_1^{(1)}}{\partial x}=-rq_2^{(1)}. \tag{6}$$

In the reduced model, the equations (5)and (6) are the equations of motion in layer 1. In a similar way, the equations of motion in layer 2 are obtained as :

$$\left(\frac{\partial}{\partial t}+\mathrm{U}_2\frac{\partial}{\partial x}\right)q_1^{(2)}+Q_{y2}\frac{\partial\psi_1^{(2)}}{\partial x}-\frac{\pi^2}{2}q_2^{(2)}\frac{\partial\psi_1^{(2)}}{\partial x}+\frac{\pi^2}{4}q_1^{(2)}\frac{\partial\psi_2^{(2)}}{\partial x}\quad-$$
$$\frac{\pi^2}{4}\psi_1^{(2)}\frac{\partial q_2^{(2)}}{\partial x}+\frac{\pi^2}{2}\psi_2^{(2)}\frac{\partial q_1^{(2)}}{\partial x}=-rq_1^{(2)}. \tag{7}$$

$$\left(\frac{\partial}{\partial t}+\mathrm{U}_2\frac{\partial}{\partial x}\right)q_2^{(2)}+Q_{y2}\frac{\partial\psi_2^{(2)}}{\partial x}+\frac{\pi^2}{4}q_1^{(2)}\frac{\partial\psi_1^{(2)}}{\partial x}-\frac{\pi^2}{4}\psi_1^{(2)}\frac{\partial q_1^{(2)}}{\partial x}=-rq_2^{(2)}. \tag{8}$$

$q \equiv$ potential vorticity, $\psi \equiv$ stream function, $r \equiv$ dissipation coefficient.

Linearising the equations (5),(6),(7) and (8) yields a slightly modified set of equations from which the linear stability of the equations can be investigated. Proposing potential vorticities and stream functions of the form below:

$$q_j^{(\ell)}=\hat{q}_j^{(\ell)}\mathrm{e}^{ik(x-ct)} \quad \text{and} \quad \psi_j^{(\ell)}=\hat{\psi}_j^{(\ell)}\mathrm{e}^{ik(x-ct)} \quad \text{for} \quad \ell=1,2; \quad j=1,2. \tag{9}$$

where x is the downstream coordinate and k is the x-direction wave number.
The superscripts in equation (9) denote layers while the subscripts denote the wave mode under consideration. The linearised forms of equations (5) and (7) can be presented in matrix form as

$$\begin{pmatrix} r+ik(\mathrm{U}_1-c)-\dfrac{ikQ_{y1}(\mathrm{K}_1^2+\mathrm{F}_2)}{\mathrm{K}_1^2(\mathrm{K}_1^2+\mathrm{F}_1+\mathrm{F}_2)} & \dfrac{-ikQ_{y1}\mathrm{F}_1}{\mathrm{K}_1^2(\mathrm{K}_1^2+\mathrm{F}_1+\mathrm{F}_2)} \\ \dfrac{-ikQ_{y2}\mathrm{F}_2}{\mathrm{K}_1^2(\mathrm{K}_1^2+\mathrm{F}_1+\mathrm{F}_2)} & r+ik(\mathrm{U}_2-c)-\dfrac{ikQ_{y2}(\mathrm{K}_1^2+\mathrm{F}_1)}{\mathrm{K}_1^2(K_1^2+\mathrm{F}_1+\mathrm{F}_2)} \end{pmatrix}\begin{pmatrix}\hat{q}_1^{(1)}\\ \hat{q}_1^{(2)}\end{pmatrix}=0 \tag{10}$$

where $\mathrm{K}_1^2=k^2+\pi^2$ and k is the x-direction wave number.

The linearised forms of equations (6) and (8) take a similar form and can be presented in matrix form in the same form as equation (10) but with K_1 swapped for $\mathrm{K}_2=k^2+2\pi^2$.

For non-trivial solutions, the determinant of the matrix in equation (10) must vanish, thus,

$$\left(r+ik(\mathrm{U}_1-c)-\frac{ikQ_{y1}(\mathrm{K}_1^2+\mathrm{F}_2)}{\mathrm{K}_1^2(\mathrm{K}_1^2+\mathrm{F}_1+\mathrm{F}_2)}\right)\left(r+ik(\mathrm{U}_2-c)-\frac{ikQ_{y2}(\mathrm{K}_1^2+\mathrm{F}_1)}{\mathrm{K}_1^2(K_1^2+\mathrm{F}_1+\mathrm{F}_2)}\right) - \left(\frac{-ikQ_{y1}\mathrm{F}_1}{\mathrm{K}_1^2(\mathrm{K}_1^2+\mathrm{F}_1+\mathrm{F}_2)}\right)\left(\frac{-ikQ_{y2}\mathrm{F}_2}{\mathrm{K}_1^2(\mathrm{K}_1^2+\mathrm{F}_1+\mathrm{F}_2)}\right)=0 \tag{11}$$

For matters of simplicity, discarding the β-effect from our consideration and also defining the shear as $\mathrm{U}_s=\mathrm{U}_1-\mathrm{U}_2$. Also considering that $\mathrm{F}_1=\mathrm{F}_2=\mathrm{F}$, then

$$\begin{aligned} Q_{y1}=\mathrm{F}\mathrm{U}_s, \quad Q_{y2}=-\mathrm{F}\mathrm{U}_s \quad \text{thus} \\ Q_{y1}+Q_{y2}=0, \quad Q_{y1}\cdot Q_{y2}=-\mathrm{F}^2\mathrm{U}_s^2 \end{aligned} \tag{12}$$

Equation (11) generates a quadratic equation in c whose solution is obtained to be

$$c=\left(\frac{-ir}{k}+\frac{1}{2}(\mathrm{U}_1+\mathrm{U}_2)\right)\pm\frac{\mathrm{U}_s}{2}\left(1-4\mathrm{F}\left(\frac{\mathrm{F}^3}{y^2}-\frac{\mathrm{F}x^2}{y^2}+\frac{x}{y}\right)\right)^{1/2} \tag{13}$$

$$\text{where} \qquad x=\mathrm{K}_1^2+\mathrm{F}, \qquad y=\mathrm{K}_1^2(\mathrm{K}_1^2+2\mathrm{F}) \quad \text{and thus}$$

$$c-\mathrm{U}_B=\frac{-ir}{k}\pm\frac{\mathrm{U}_s}{2}\left(\frac{\mathrm{K}_1^2-2\mathrm{F}}{\mathrm{K}_1^2+2\mathrm{F}}\right)^{1/2}. \tag{14}$$

Thus c is generally complex and can be written as $c = c_r + ic_i$ where c_r and c_i are the real and imaginary parts of c respectively. In case the term in the last parentheses vanishes, then the dispersion relation reduces to

$$c = \left(\frac{-ir}{k} + \mathrm{U}_B\right) \qquad \text{where} \quad \mathrm{U}_B = \frac{1}{2}(\mathrm{U}_1 + \mathrm{U}_2), \quad \text{the barotropic flow.} \tag{15}$$

It is also observed that the decay of the perturbation is proportional to the dissipation in the system and is higher for lower wave numbers. In this case, the shear does drop out of the dispersion relation rendering the dissipation, r, and the magnitude of the barotropic flow as the parameters governing the flow dynamics in the channel under study.

However if $\mathrm{K}_1 < (2\mathrm{F})^{1/2}$, then the last parentheses in equation (14) also contribute to the complex part of c and in turn the shear, U_s and the Froude number, F become effective parameters of the system.

In the following, simulations will be conducted in two main categories; the first being the case when the dissipation, $r = O(1)$ and the second being the case when the dissipation is almost zero in the system i.e $r = O(\Delta)$ for very small Δ.

(i) $r = O(1)$
In this case, the only way of having a growing instability is that $2\mathrm{F} > \mathrm{K}_1^2$ and the whole term in the parentheses must be large enough to outweigh the decay term, $\frac{-ir}{k}$. This yields the relation for the marginal condition on U_s in order to have a growing instability. With values selected as $r = 4.6, \mathrm{F} = 40, l = \pi \quad \text{and} \quad 0 < k < 5.0$

$$\mathrm{U}_s = \frac{2r}{k}\left(\frac{2\mathrm{F} + \mathrm{K}_1^2}{2\mathrm{F} - \mathrm{K}_1^2}\right)^{1/2} \tag{16}$$

(ii) $r = O(\Delta)$
With r small, the marginal curve is given in terms of the parameter, F and takes the form

$$\mathrm{F} = \frac{\mathrm{K}_1^2}{2} = \frac{k^2 + l^2}{2} \tag{17}$$

F thus has a parabolic form with a minimum at $k = 0$ and takes the form below:

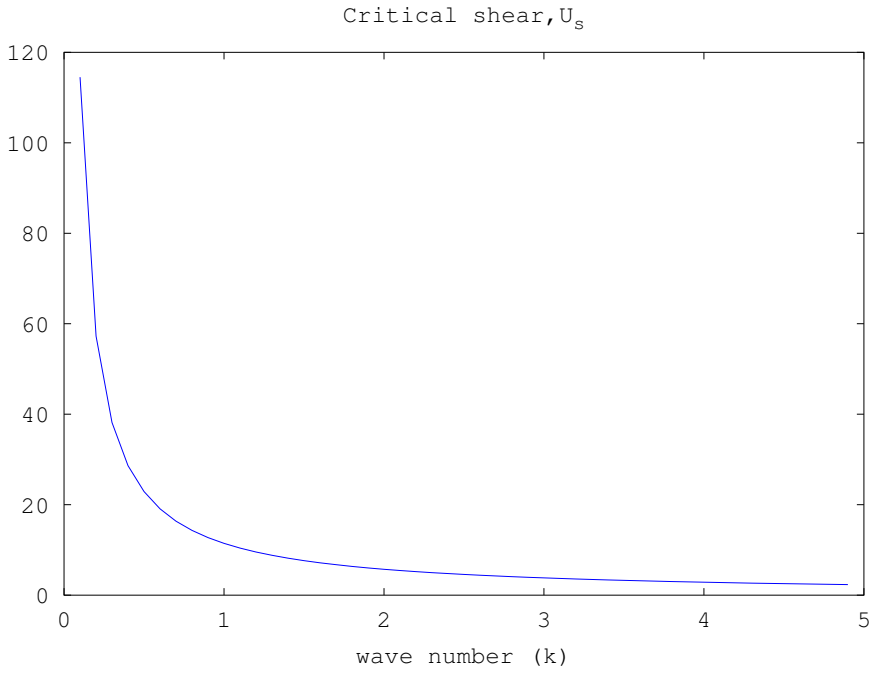

Numerical Simulations and Results

The case $r = O(1)$

The model set up is such that the system is slightly above its neutral criticality. The barotropic velocity in the channel is set at $U_B = 13.125$ and the most unstable mode is to be k = 4.34 . The parameter values of the model when neutrally critical and those used in the numerical simulation are given in table 1.

Table 1: Model parameters used for the case $r = O(1)$

Parameter	Symbol	Critical values	Simulation value
Shear	U_s	3.00	3.25
Froude number	F	40.0	40.0
Dissipation	r	4.60	4.60

With the shear slightly increased above the neutrally critical value of the shear, an initial perturbation is set up at the entrance of the channel (i.e at $x = 0$) and it's downstream development with time is studied. The boundary conditions are such that at the channel entrance, a perturbation, $A_o \sin(\omega t)$ with frequency $\omega = kU_B$ is seeded. At the end of the channel, spongy boundaries are considered such that whatever is incident on the wall, goes in and none of it is reflected back into the channel. The meridional walls are rigid and the potential vorticities there are zero*.

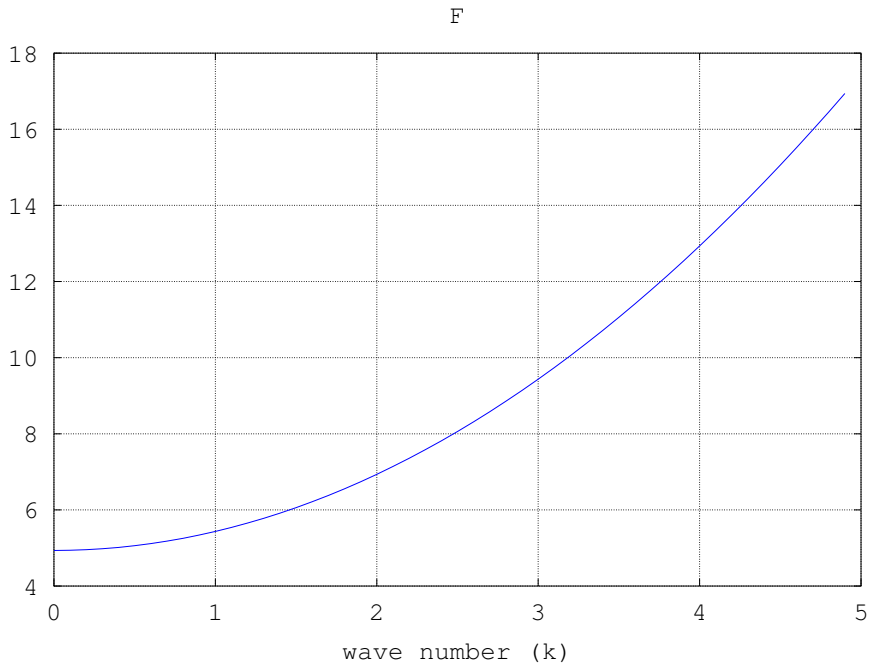

Discussion

It's observed that to first order, the solution has both the barotropic and baroclinic modes on $\sin(\pi y)$ as the leading terms of the solution to the nonlinear set of equations (5,6,7 and 8). The leading terms of the solution exhibit the oscillations of the initial perturbation imposed at the entrance of the channel (see figures 1 and 3) all the way downstream. The amplitude of the perturbation grows initially until it reaches a finite amplitude and thereafter momentarily stabilises before eventually decaying off to zero. The stabilisation in growth of the perturbation at finite amplitude is longer downstream.

In all cases and for all the modes considered, it is observed that the part of the growing perturbation behind the front reaches finite amplitude before saturation such that in the regions ahead of the front, the amplitude of the perturbation remains constant in the vicinity of the front and decays quite quickly away from the front downstream. The slightly unique cases amongst the modes considered in this study are those of the baroclinic and barotropic modes on $\sin(2\pi y)$ which appear to be relatively smooth compared to the leading order terms. With the exception of a few oscillations whose amplitudes are still small near the channel entrance, any information about the oscillatory nature of the perturbation is lost downstream and the resulting correction to the mean flow is of a largely smooth structure.

Behind the front, wiggles are observed in the spatial and temporal structure of the perturbation before finally reaching finite amplitude in the vicinity of the front. Ahead of the front, the perturbation has already reached finite amplitude and therefore remains constant (for longer time scales) or immediately decays (for shorter time scales) ahead of the front. This is in agreement with Pedlosky (2011) who highlighted that the correction to the mean flow carries the oscillatory information of the perturbation only behind the front

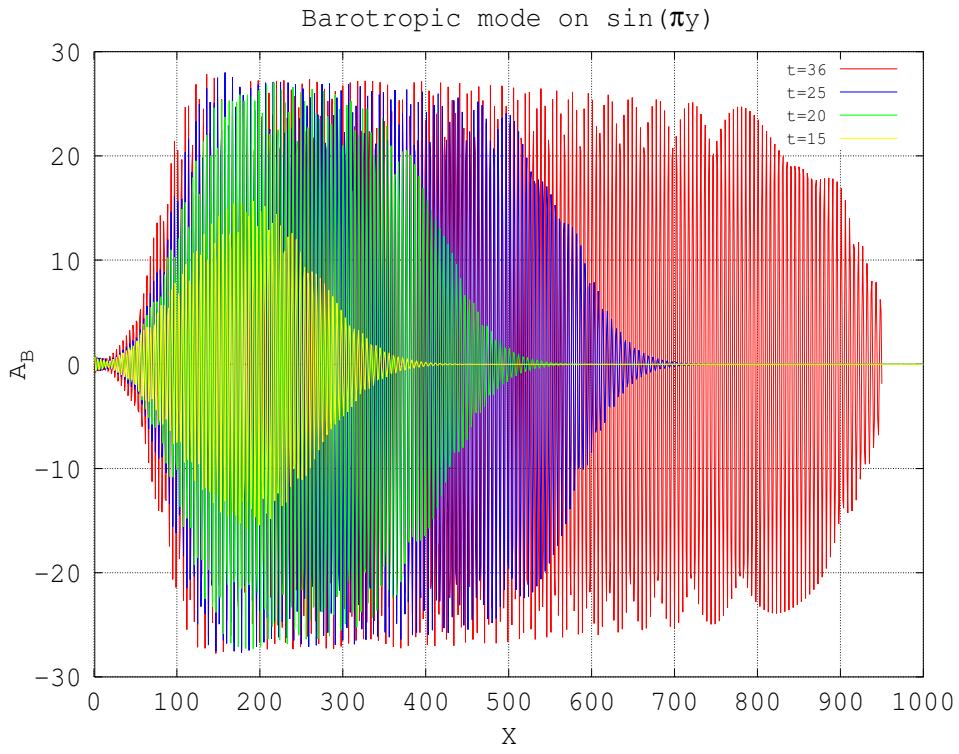

Figure 1: Snapshots of the barotropic potential vorticity on the sin(πy) mode with $U_s = U_{so} + 0.25$ and $r = r_o$

during which time the perturbation also attains finite amplitude. In that study, they also observe that ahead of the front, the structure is basically a smooth one with the perturbation having reached finite amplitude.

However, it is also observed that the baroclinic mode on sin(2πy) is also the largest of the projections on the sin(2πy) modes. This is consistent with the results obtained by (Pedlosky, 2011) which highlighted that the first order correction to the mean flow was fully baroclinic.

However, the non-linear simulations carried out in this study reveal that there's a small contribution to the mean flow correction by the barotropic component carried by the barotropic component on the sin(2πy) mode. It's the smallest of all the components but it is worth mentioning that although the asymptotic approach adopted using the finite amplitude model in Pedlosky (2011) fails to capture this contribution, it is not necessarily zero as observed in figure 2.

A probable explanation as to why the asymptotic approach shows that the sin($2\pi y$) barotropic mode does not contribute to the mean flow correction could be that as observed from figure (2), the average of this mode over a period is zero. So, it could be asserted that the reason for the failure to capture to this mode in the theory is not because it's so small in magnitude but it's because it vanishes on average. More interestingly for all time, apart

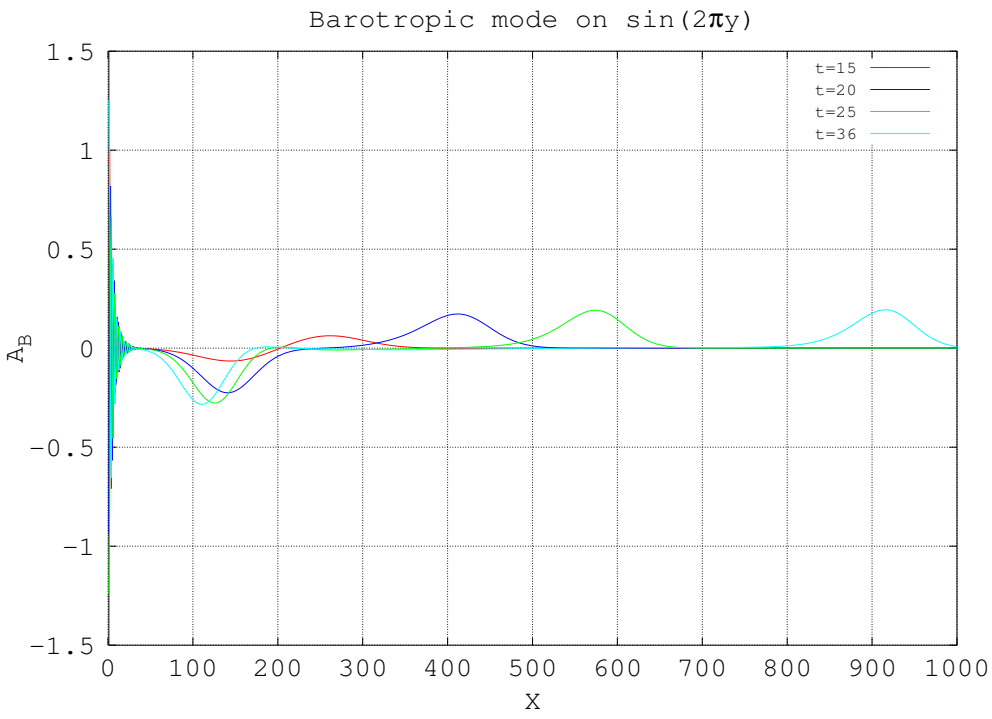

Figure 2: Snapshots of the baroclinic potential vorticity on the sin(2πy) mode with $U_s = U_{so} + 0.25$ and $r = r_o$

from the initial transients, the $\sin(2\pi y)$ barotropic mode manifests as a periodic oscillation whose average over a period vanishes.

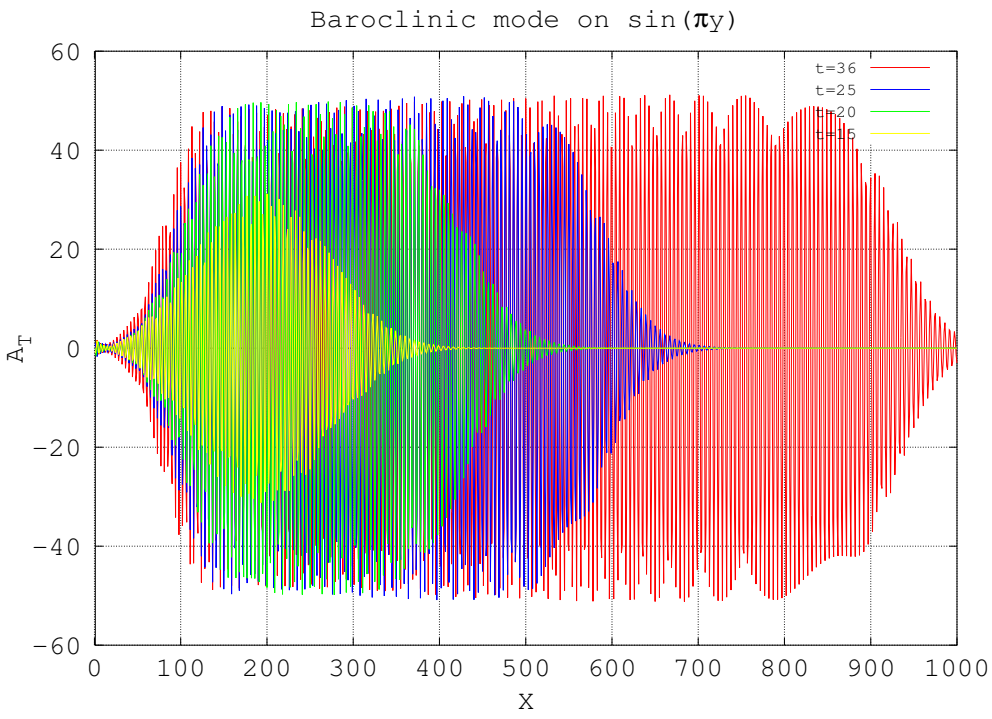

Figure 3: Snapshots of the baroclinic potential vorticity on the sin(πy) mode with $U_s = U_{so} + 0.25$ and $r = r_o$

The case r=O(Δ)

Table 2: Model parameters used for the case $r = O(\Delta)$

Parameter	Symbol	Critical values	Simulation value
Shear	U_s	1.30	1.30
Froude number	F	4.9348	4.9348 + 0.02
Dissipation	r	0.001	0.001

The barotropic flow in this case is reduced to $U_B = 1.65$ and the most unstable mode corresponds to the wave number $k = 0.15$.

Several simulations are carried out with various degrees of super criticalities (i.e for increasing values of Δ) and the results are presented in the following figures. For most values of Δ, the flow does not seem to change significantly but it happens that as Δ increases, more features emerge ahead of the front for longer times.

As the theory predicts, the largest component of the correction to the leading order solution is baroclinic (the sin$2\pi y$ baroclinic mode). However, the fully non-linear solution shows that a barotropic contribution is also present. The latter is initially small (≈ 0) but develops with time until it is one order of magnitude lower than the baroclinic correction.

Discussion

It's observed that at the leading order, the dominant part of the flow is the $\sin\pi y$ barotropic mode. The $\sin\pi y$ baroclinic mode is lower than the former but it's significantly appreciable. This is in agreement with the findings of Pedlosky (2011) that showed that in this regime, the leading order solution is the $\sin\pi y$ mode and that its baroclinic counterpart is an order of magnitude lower. Although not as much as an order of magnitude, the fully nonlinear solutions strongly yield similar results.

At the next order, the major correction component to the mean flow is found to be fully baroclinic (i.e the $\sin 2\pi y$ baroclinic mode). The $\sin 2\pi y$ barotropic mode is consistently zero throughout the time of the simulation. This is also in agreement with the findings from the multi-scale asymptotics which yielded that the correction to the mean flow is fully baroclinic.

Increasing the degree of super criticality leads to a complete break down of the predictions of the linear and weakly non-linear theory. In this case, at leading order, the dominant term is the $\sin\pi y$ baroclinic mode as opposed to the $\sin\pi y$ barotropic mode predicted by theory. Also, at the next order, the barotropic correction to the mean flow becomes appreciable which is, of course, another difference from the case considered when the dynamics are slightly super critical. The other remarkable feature that emerges with increasing levels of supercriticalities is that the features formed ahead of the front become more apparent and highly variable downstream as one would expect when the non-linearirities in the system are at full operation.

In conclusion, the findings from this study qualitatively show that the degree of dissipation in the system is a major determinant of the dynamics of the flow. When the system is substantively dissipative, the marginal curve is given in terms of the shear and the dominant correction component to the mean flow is largely baroclinic. In the case when the dissipation is so small, the marginal curve is expressed in terms of the parameter, F - the Froude number. In this case, the lowest order compnent is found to be barotropic and the correction is fully baroclinic.

For further study, it would be meaningful to consider using a periodic channel so that the flow statistics can be obtained with a good degree of accuracy to enable giving a quantitative account of the dynamics of the flow and how the different components exchange the energy in both spatial and temporal considerations. Of course, inclusion of the $\beta-$ effect would also serve the purpose of comparing the results obtained to what happens in a real oceanographic scenario.

Acknowledgement

My sincere thanks go to the directors of the Geophysical Fluid Dynamics (GFD) summer school of 2014 for giving me the opportunity to be one of the fellows this year. It has been such a remarkable experience with talks and academic discussions with scientists from several institutions. From the principle lectures offered by Professors Kerry Emanuel and Geoffery Vallis to the research project, every moment has been remarkable and unforgettable.

Sincere gratitude also to my advisor Prof. Joseph Pedlosky of Woods Hole Oceanographic Institution who gave the academic direction of the project. The prompt email replies which had to be made at times late in the night or very early in the morning depicted tremendous commitment and willingness to help me accomplish the project. Thanks a lot, Joe.

I would also like to acknowledge the much welcomed assistance and support offered by Professor Glenn Flierl of Massachussetts Institute of Technology who not only provided regular guidance during the course of the project but also helped in providing the numerical code used in the study. Glenn's regular explanations made such a huge impact toward a better understanding of the problem studied and in turn shaped the direction of the study. Equally important was the support and academic guidance given by Stephen Meacham throughout the study. Thanks so much for all your efforts in seeing this project come to its completion.

References

Pedlosky, J. (1970). Finite-amplitude baroclinic waves. *Journal of Atmospheric Sciences*, 27:15–30.

Pedlosky, J. (2011). The nonlinear downstream development of baroclinic instability. *Journal of Marine Research*, 69:705–722.

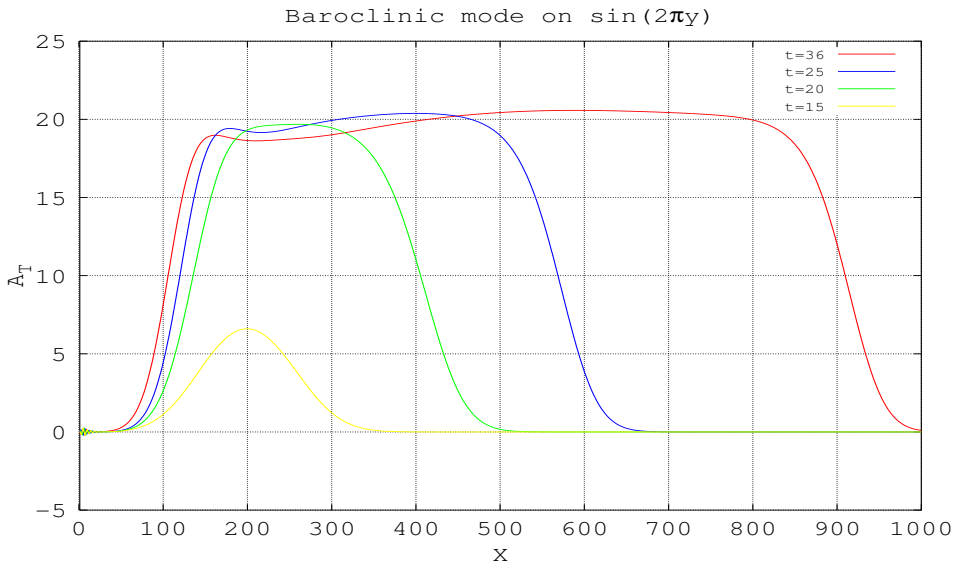

Figure 4: Snapshots of the baroclinic potential vorticity on the sin(2πy) mode with $U_s = U_{so} + 0.25$ and $r = r_o$

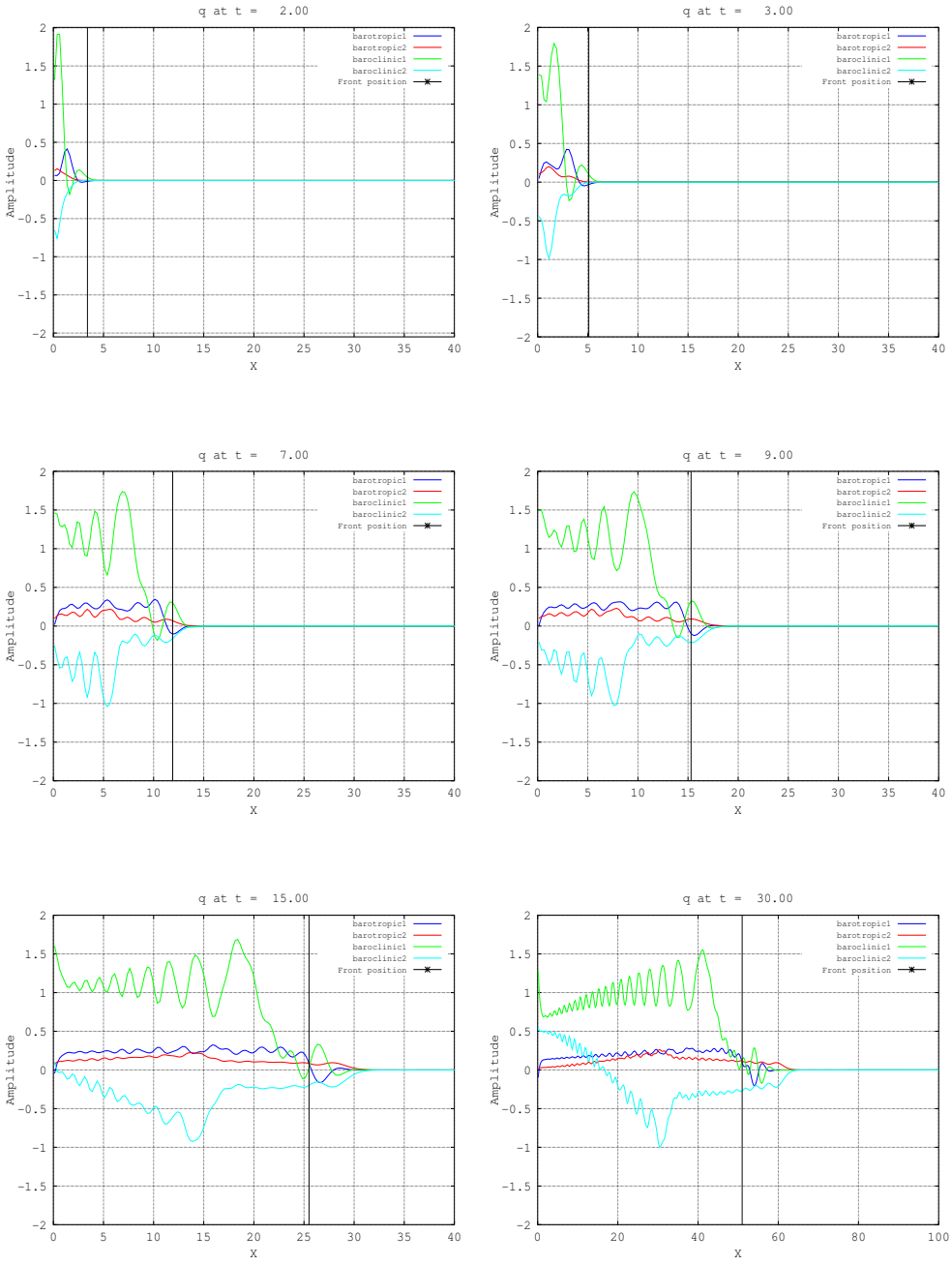

Figure 5: Snapshots of the barotropic and baroclinic potential vorticities. $\Delta = 0.02$

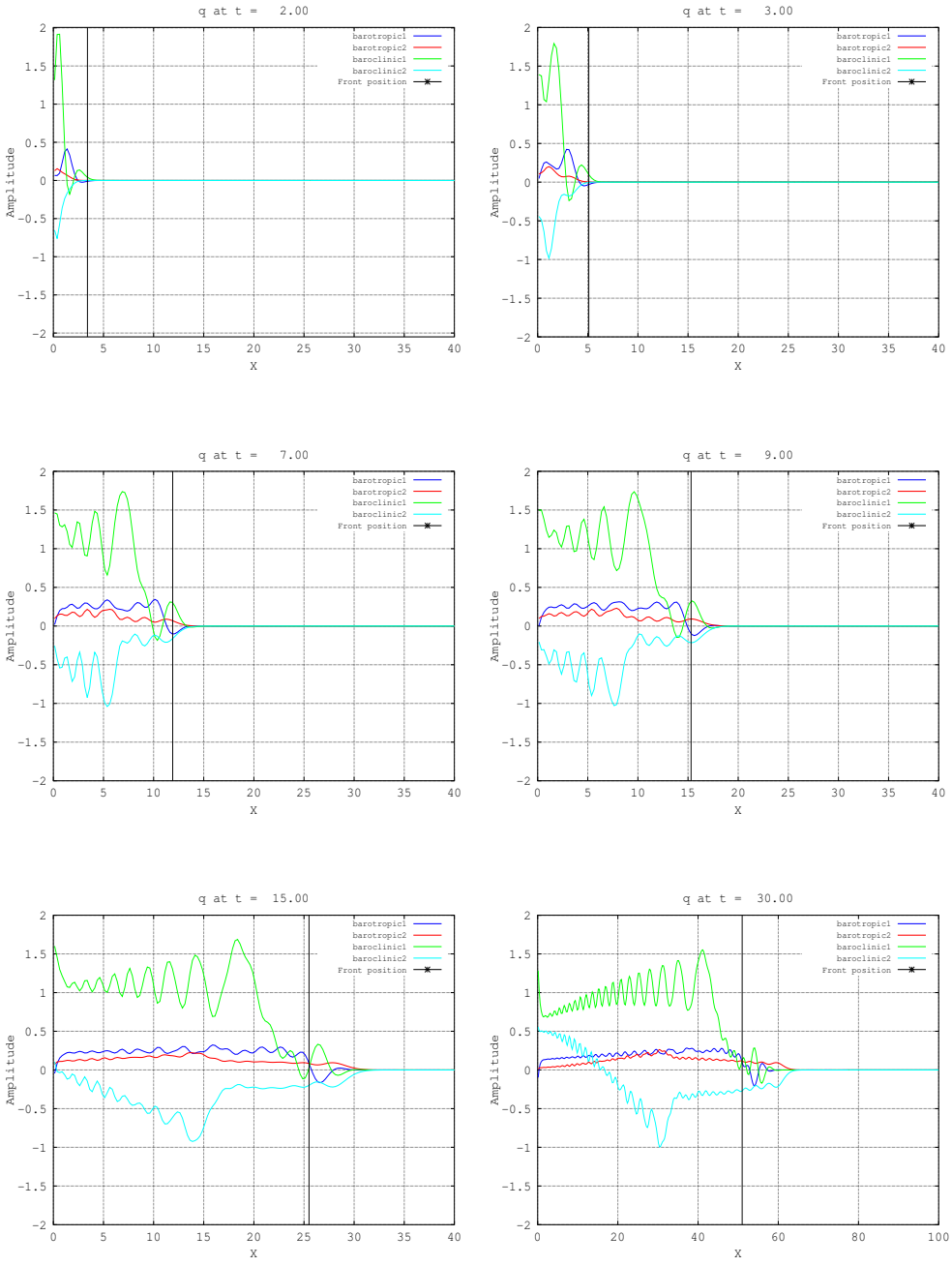

Figure 6: Snapshots of the barotropic and baroclinic potential vorticities. $\Delta = 0.05$

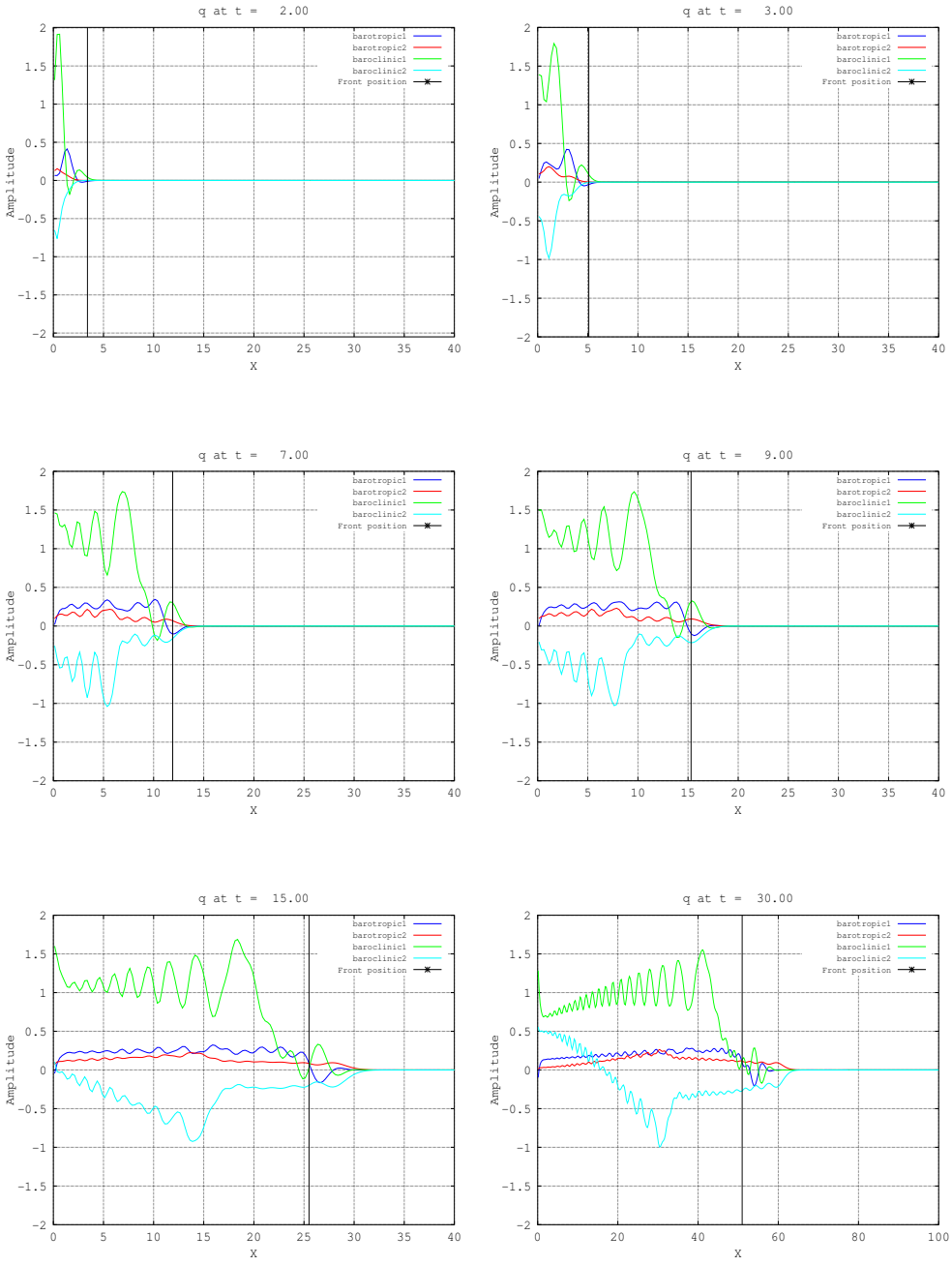

Figure 7: Snapshots of the barotropic and baroclinic potential vorticities. $\Delta = 0.1$

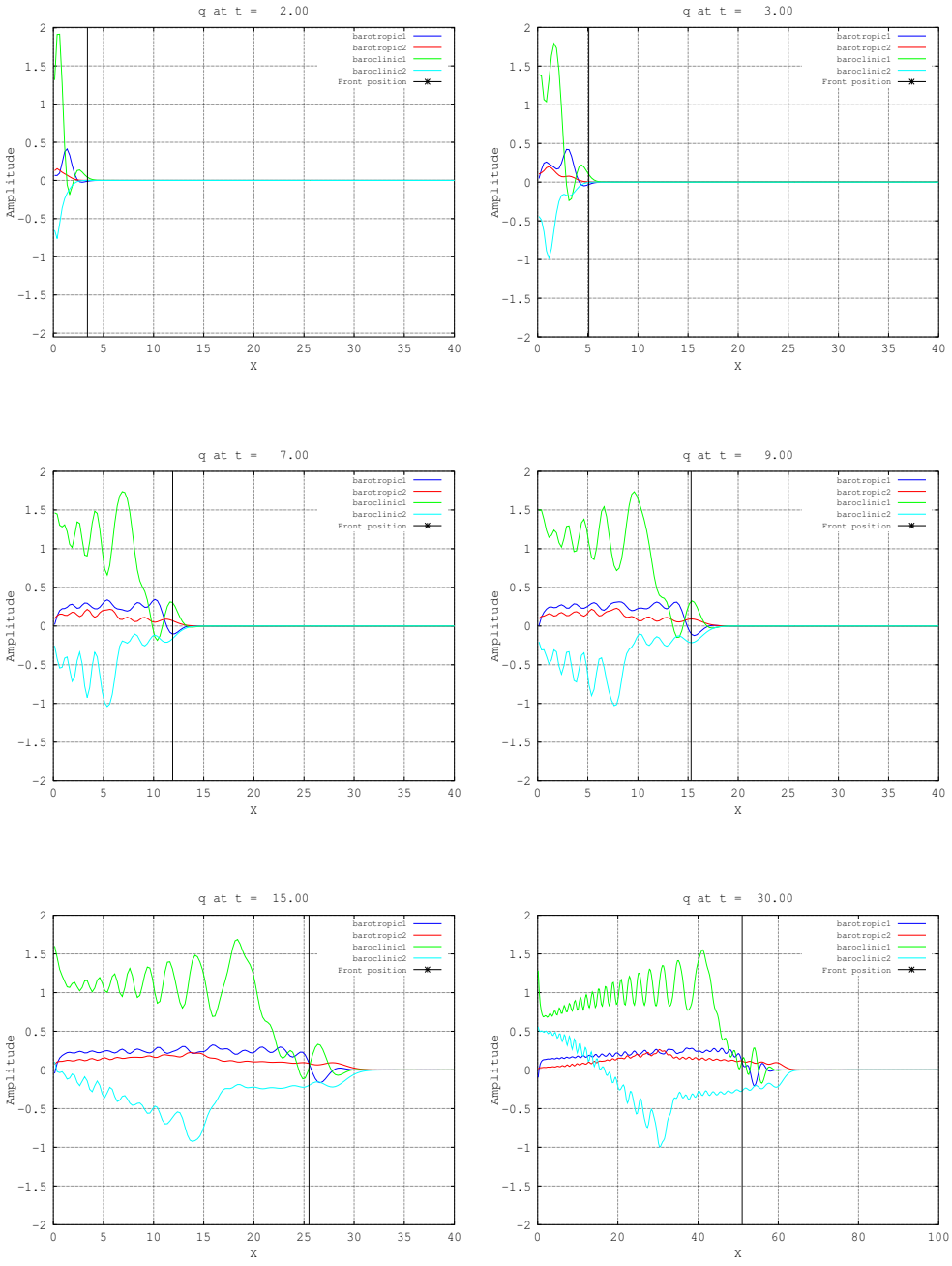

Figure 8: Snapshots of the barotropic and baroclinic potential vorticities. $\Delta = 0.7$